Stem Cell Reports
Article
OPEN ACCESS

Reduced Self-Diploidization and Improved Survival of Semi-cloned Mice Produced from Androgenetic Haploid Embryonic Stem Cells through Overexpression of *Dnmt3b*

Wenteng He,[1,6] Xiaobai Zhang,[1,6] Yalin Zhang,[1] Weisheng Zheng,[1] Zeyu Xiong,[3] Xinjie Hu,[1] Mingzhu Wang,[1] Linfeng Zhang,[1] Kun Zhao,[1] Zhibin Qiao,[1] Weiyi Lai,[4] Cong Lv,[4] Xiaochen Kou,[1] Yanhong Zhao,[1] Jiqing Yin,[1] Wenqiang Liu,[1] Yonghua Jiang,[5] Mo Chen,[1] Ruimin Xu,[1] Rongrong Le,[1] Chong Li,[1] Hong Wang,[1] Xiaoping Wan,[1] Hailin Wang,[4] Zhiming Han,[2] Cizhong Jiang,[1,*] Shaorong Gao,[1,*] and Jiayu Chen[1,*]

[1]Clinical and Translation Research Center of Shanghai First Maternity & Infant Hospital, Shanghai Key Laboratory of Signaling and Disease Research, School of Life Sciences and Technology, Tongji University, Shanghai 200092, China
[2]State Key Laboratory of Stem Cell and Reproductive Biology, Institute of Zoology, Chinese Academy of Sciences, Beijing 100101, China
[3]Key Laboratory for Major Obstetric Diseases of Guangdong Province, Key Laboratory of Reproduction and Genetics of Guangdong Higher Education Institutes, The Third Affiliated Hospital of Guangzhou Medical University, Guangzhou 510150, China
[4]The State Key Laboratory of Environmental Chemistry and Ecotoxicology, Research Center for Eco-Environmental Sciences, Chinese Academy of Sciences, Beijing 100085, China
[5]Center for Genomic and Personalized Medicine, Guangxi Medical University, Nanning, Guangxi 530021, China
[6]Co-first author
*Correspondence: czjiang@tongji.edu.cn (C.J.), gaoshaorong@tongji.edu.cn (S.G.), chenjiayu@tongji.edu.cn (J.C.)
https://doi.org/10.1016/j.stemcr.2017.12.024

SUMMARY

Androgenetic haploid embryonic stem cells (AG-haESCs) hold great promise for exploring gene functions and generating gene-edited semi-cloned (SC) mice. However, the high incidence of self-diploidization and low efficiency of SC mouse production are major obstacles preventing widespread use of these cells. Moreover, although SC mice generation could be greatly improved by knocking out the differentially methylated regions of two imprinted genes, 50% of the SC mice did not survive into adulthood. Here, we found that the genome-wide DNA methylation level in AG-haESCs is extremely low. Subsequently, downregulation of both *de novo* methyltransferase *Dnmt3b* and other methylation-related genes was determined to be responsible for DNA hypomethylation. We further demonstrated that ectopic expression of *Dnmt3b* in AG-haESCs could effectively improve DNA methylation level, and the high incidence of self-diploidization could be markedly rescued. More importantly, the developmental potential of SC embryos was improved, and most SC mice could survive into adulthood.

INTRODUCTION

Haploid embryonic stem cells (haESCs) are a special kind of ESCs that possess a single set of chromosomes and act as a unique tool for forward and reverse genetic screens as well as for understanding the regulation of the mammalian genome network (Elling et al., 2011; Wutz, 2014). The first haESC line was derived from medaka fish embryos in 2009 (Yi et al., 2009). Since then, parthenogenetic (Elling et al., 2011; Leeb and Wutz, 2011) and androgenetic (AG) murine haESCs have been successfully established by applying a 2i (CHIR99021 and PD0325901) culture system along with continuous fluorescence-activated cell sorting (FACS) (Li et al., 2012; Nichols and Smith, 2011; Yang et al., 2012; Ying et al., 2008). Moreover, AG-haESCs have been demonstrated to replace sperm and produce viable and fertile progeny after intracytoplasmic injection into mature oocytes (Li et al., 2012; Yang et al., 2012). Recently, *Macaca fascicularis* monkey haESCs (Yang et al., 2013) and human parthenogenetic haESCs were established (Sagi et al., 2016; Zhong et al., 2016b). However, haESCs are prone to self-diploidization during prolonged culture (Kaufman et al., 1983; Leeb et al., 2012). In addition, the efficiency for generating full-term, live semi-cloned (SC) animals was low (0%–4% in mouse and 0%–1.2% in rat), and approximately 50% of the SC mice exhibited growth retardation and died shortly after birth (Li et al., 2012, 2014; Yang et al., 2012). A recent study indicated that a double knockout (DKO) of differentially methylated regions (DMRs) of *H19* and *Gtl2* in AG-haESCs could markedly improve the birth rate of SC mice to 14.4%–22.4% (Zhong et al., 2015), but the definite survival rate to adulthood for these mice was not clearly described. In addition, a recent report indicated this DKO was not beneficial enough (Li et al., 2016).

DNA cytosine methylation is one of the most important modifications in the epigenetic genome and plays essential roles in various cellular processes, including genomic imprinting, X chromosome inactivation, retrotransposon silencing, as well as regulation of gene expression and embryogenesis (Bird, 2002; Reik et al., 2001). In mammals, most methylated CpGs are concentrated on repetitive

sequences and in the DMRs of many genes, especially imprinted genes (Zvetkova et al., 2005). Major and minor satellite repeats are mostly located in acrocentric chromosomes that associate with centromeres and function in correct chromatid segregation and cell division (Guenatri et al., 2004). Long interspersed nuclear element-1 (LINE-1) and intracisternal A particles (IAP) are retrotransposons whose aberrant activation can induce genomic instability (Lane et al., 2003; Martinez et al., 2012). Proper methylation is necessary for suppressing the activity of retrotransposons and maintaining genome stability across generations in germ cells (Crichton et al., 2014). However, the methylation status of repetitive sequences in haESCs has not been described. Imprinted genes are monoallelic genes that are expressed according to their parental origin, and they play important roles in normal development. For instance, the paternally expressed *Igf2* gene is a positive regulator of fetal growth, and its reduction results in growth restriction (Plasschaert and Bartolomei, 2014). The maternally expressed *Gtl2* (*Meg3*) is regulated by intergenic germline-derived DMR (Plasschaert and Bartolomei, 2014), and it plays roles in various human cancers (Yan et al., 2016). Lower *Igf2* expression and higher *Gtl2* expression were found in both AG-haESCs and growth-retarded SC mice (Yang et al., 2012; Zhong et al., 2015).

The addition of methyl groups to cytosine residues is catalyzed by DNA methyltransferases (DNMTs): Dnmt1, Dnmt3a, and Dnmt3b. Dnmt1 is required for methylation maintenance during cell division (Hirasawa et al., 2008). In contrast, Dnmt3a and Dnmt3b are referred to as *de novo* methyltransferases and are responsible for the creation of new methyl groups on the cytosine residues of unmethylated CpG sites (Okano et al., 1998). In addition, murine ESCs (mESCs) lacking both Dnmt3a and Dnmt3b cause hypomethylation of satellite repeats, IAP, and unique DMRs (Okano et al., 1999). In animal models, mice lacking either *Dnmt1* or *Dnmt3b* exhibit embryonic lethality, while *Dnmt3a*$^{-/-}$ mice exhibit postnatal growth retardation and die at approximately 4 weeks of age (Li et al., 1992; Okano et al., 1999).

In the present study, we observed global hypomethylation of AG-haESCs generated in our study and others, which affects the methylation levels at repetitive sequences as well as the DMRs of certain imprinted genes. Furthermore, we found certain methylation-related genes, especially *Dnmt3b*, that are obviously downregulated. Importantly, overexpression of *Dnmt3b* can effectively increase genomic methylation levels, restoring methylation in repetitive sequences and mitigating the self-diploidization of AG-haESCs. More importantly, the developmental potential of SC embryos was promoted, and the survival rate of DKO SC mice can be remarkably improved, even reaching up to 90%.

RESULTS

Establishment of Androgenetic Haploid Embryonic Stem Cells

Two genetic background mouse strains, 129Sv and C57BL/6 (*Oct4*-GFP transgenic mouse), were selected as sperm donors. AG haploid embryos were successfully produced by injecting one sperm head into an enucleated oocyte according to the standard protocol (Figure 1A) (Li et al., 2012; Yang et al., 2012). In total, 778 embryos (264 in the 129Sv background and 514 in the C57/*Oct4*-GFP background) were reconstructed, and 156 embryos finally developed to the blastocyst stage, with an efficiency comparable with that of a previous report (Figures 1B, 1C, and 1F) (Yang et al., 2012). These AG blastocysts were then seeded on feeders and AG-haESC lines could finally be maintained under a serum/leukemia inhibitory factor (LIF)+2i culture system after FACS (Figures 1D–1F, S1A, and S1B). All these AG-haESC lines could retain the haploid properties (19 + X chromosomes) after more than 60 passages (Figures 1G, S1C, and S1D) and had normal telomere signals (Figure 1G).

All six AG-haESC lines presented colony-like morphology with smooth, clear edges, similar to that of diploid mESCs (2n mESCs) and previously reported AG-haESCs (Yang et al., 2012) (Figures 1G, S1B, and S1E). Both quantitative real-time qPCR and immunofluorescence (IF) staining analysis showed that pluripotent markers, including *Oct4*, *Sox2*, *Dppa4*, *Utf1*, *Klf4*, and *Nanog*, as well as the surface marker SSEA1, were highly expressed in AG-haESCs (Figures 1H, S1F, and S1G). Moreover, all the tested AG-haESCs could generate teratomas with cells from three germ layers in the immune-deficient nude mice (Figures S1H and S1I). In summary, all six of these AG-haESC lines derived from two genetic backgrounds have pluripotency similar to that of normal 2n mESCs.

Production of Semi-cloned Mice by AG-haESCs

We next tested whether these AG-haESC lines could replace sperm to fertilize oocytes after performing intracytoplasmic AG-haESCs injection (ICAI) (Figure 2A) (Li et al., 2012; Yang et al., 2012). Specifically, the AG-haESCs were first synchronized at metaphase and smaller cells were selected and injected into the MII-phase oocytes (Figure 2A). Several hours later, the second polar body and the pseudopolar body were excluded, and these reconstructed embryos could further develop into blastocysts at a rate of 45%, which is comparable with that of previously reported cells (Figures 2B, 2C, S2A, and S2B) (Yang et al., 2012).

We next tested the *in vivo* developmental potential of these reconstructed embryos by transferring embryos at

Please cite this article in press as: He et al., Reduced Self-Diploidization and Improved Survival of Semi-cloned Mice Produced from Androgenetic Haploid Embryonic Stem Cells through Overexpression of..., Stem Cell Reports (2018), https://doi.org/10.1016/j.stemcr.2017.12.024

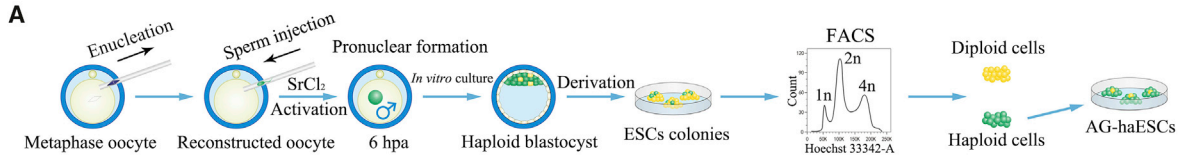

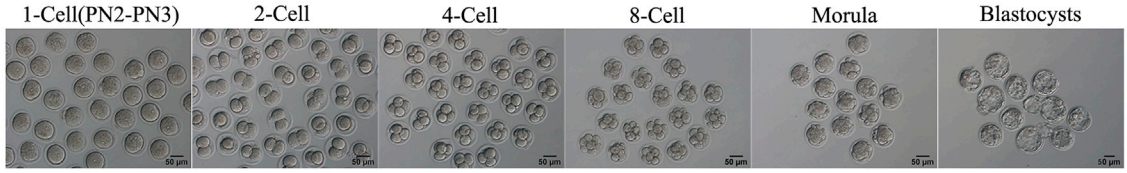

C

Donor sperms	Replicates	No. of manipulated	No. of 2-Cell (%)	Blastocyst (% of manipulated)	ESC lines obtained (% of blastocysts)	AG-haESCs obtained (% of ESC lines)	Names of AG-haESCs
129Sv	1	92	87 (94.57)	14 (15.22)	2 (14.29)	1(14.29)	A129-2
	2	101	92 (91.09)	20 (19.80)	3 (15.00)		
	3	71	65 (91.55)	12 (16.90)	2 (16.67)		
	Subtotal	264	244(92.42)	46 (17.42)	7 (15.22)		
C57(*Oct4*-GFP)	1	148	126(85.14)	30 (20.27)	5 (16.67)	5(26.32)	AOS-13 to AOS-17
	2	204	193(94.61)	37 (18.14)	7 (18.92)		
	3	162	147(90.74)	43 (26.53)	7 (16.28)		
	Subtotal	514	466(90.66)	110(23.60)	19(17.27)		

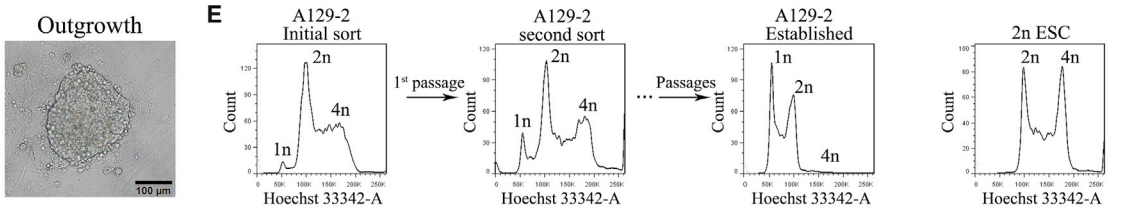

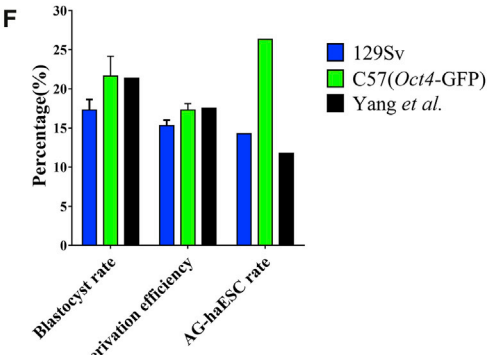

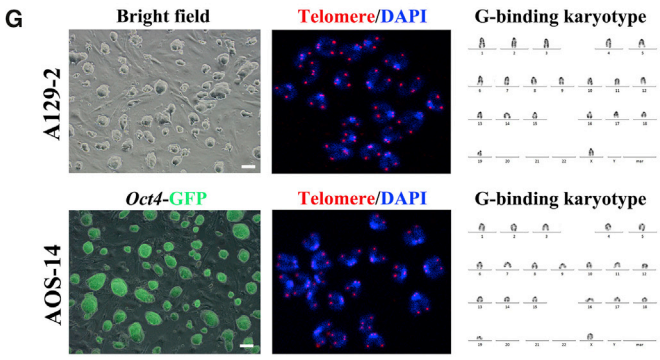

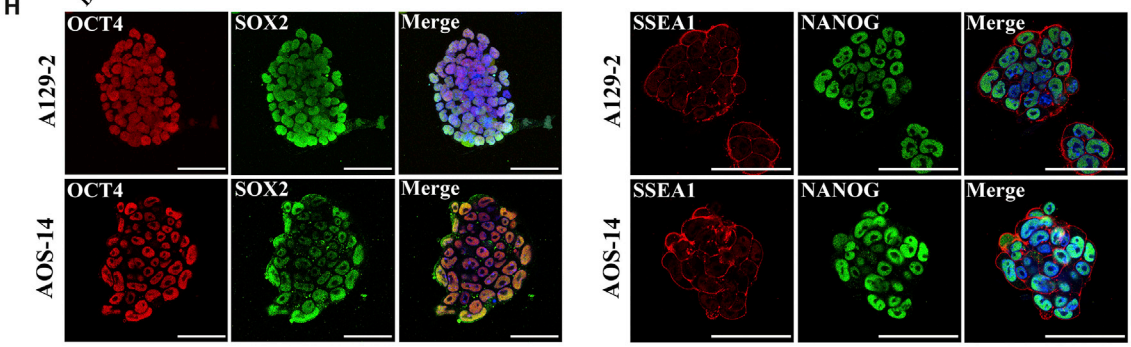

(legend on next page)

the two-cell or blastocyst stage into pseudopregnant females. There were no significant differences among the A129-2 cells, the AOS cells, and the previously reported AG-haESCs (Yang et al., 2012) in the early embryo developmental rate (Figures 2D and S2A). In addition, all the AOS cell lines could contribute to germ cells of SC fetuses (Figure 2E). Moreover, both A129-2 and AOS-14 cells could support full-term development of the SC mice with efficiency comparable with that of the tested control AG-haESCs (Yang et al., 2012), and these mice could deliver offspring after mating with a C57 male mouse (Figures 2D, 2F, 2G, S2A, S2C, and S2D) (Li et al., 2012; Yang et al., 2012).

Transcriptome Analysis of AG-haESCs

To determine the mechanism underlying the extremely low birth rate of SC mice generated by ICAI, we performed RNA sequencing (RNA-seq) analysis on three of the AG-haESC lines (A129-2, AOS-14, and AOS-16) by collecting cells in the G0/G1 phase after FACS. Round spermatids, diploid XX, and XY ESCs cultured in the 2i system were used as controls. The results indicated that the AG-haESCs showed an ES-like expression pattern, which was quite different from round spermatids (Figures 3A, S3A, and S3B). In addition, female ESCs seemed more similar between each other (Figures 3A and S3A). Interestingly, certain pluripotency genes were uniquely expressed in AG-haESCs (Figures S3C and S3D). Moreover, our AG-haESCs were highly correlated with the previously reported AG-haESC (AGH-OG3) (Figures 3A, S3A, and S3B) (Zhong et al., 2015).

Volcano plots of p value ($-\log_{10}$ scale) versus fold change ($\log_2$ scale) showed that certain genes were differentially regulated in the AG-haESCs (X) compared with the diploid ESCs (XX) (Figures 3B and 3C). Specifically, gene ontology (GO) analysis indicated that most of the upregulated genes are correlated with spermatogenesis, meiosis, and the spermatid development process, which is closely related to their function as gametes to birth SC mice (Figure 3D).In addition, GO analysis on the downregulated genes indicated abnormities in cell proliferation as well as cell growth (Figure 3E). Moreover, we clustered the differentially expressed genes into four groups, and the significantly enriched GO terms also highly correlated with the characteristics of AG-haESCs (Figures S3E and S3F).

Interestingly, although a few methyltransferase-, methylation cofactor-, and demethylase-related genes are differentially expressed between male and female (X and XX) ESCs, haploid ESC (X) itself has unique expression patterns in certain methylation-related genes (Figures 3F and S3G). For example, *Dnmt3b* as well as *Tet1* and *Tet2* was further downregulated in all the AG-haESCs, whereas *Dnmt3a*, *Dnmt3l*, *Suv39h1*, and *Ehmt1* were upregulated when comparing with female 2n ESCs (Figures 3F and S3G). In addition, certain imprinted genes and cell-cycle-related genes were obviously mis-regulated (Figures 3G and 3H).

Reduced Methylation Levels in the AG-haESCs

We next focused on the *de novo* methyltransferase *Dnmt3b*, which was significantly downregulated in all the AG-haESC lines (Figures 3F and S3G). qPCR and western blot analysis both confirmed the remarkable deficiency of *Dnmt3b* in all the AG-haESCs (Figures 4A, 4B, and S4A). Moreover, UHPLC-MRM-QQQ (ultra-high-performance liquid chromatography-multiple reaction monitoring-triple quadrupole) analysis further demonstrated a significant reduction in global 5-methylcytosine (5 mC) levels in the AG-haESCs when comparing with 2n ESC (XX), 2n ESC (XY), and round spermatids (Figure 4C). For instance, the 5 mC level in A129-2 cells was less than one-fourth of that in 2n ESC (XX) and one-sixth of that in 2n ESC (XY). In addition, despite the female ESCs (both X and XX) showing 5 mC recovery after withdrawal of 2i, both cells still showed hypomethylation (Figure S4B). In addition, IF staining confirmed the reduced 5 mC signal in the AG-haESCs (Figure 4D). Most importantly, the SC mice produced from the AG-haESCs also showed obvious hypomethylation (Figure 4E). Therefore, the AG-haESCs possessed unique levels of methylation, which were quite different from those of round spermatids even though both could generate live pups. Moreover, this hypomethylation could be inherited with development of the SC fetus.

Figure 1. Derivation and Characterization of AG-haESCs

(A) Schematic diagram for derivation of AG-haESCs. hpa, hours post activation.

(B) *In vitro* development of androgenetic embryos with 129Sv background.

(C) *In vitro* development efficiency of androgenetic embryos as well as the derivation efficiency of AG-haESCs.

(D) Outgrowth derived from an androgenetic blastocyst.

(E) Enrichment of haploid ESCs by FACS. The diploid ESC (2n ESC) is represented as a control.

(F) Comparison of the *in vitro* development efficiency of androgenetic blastocysts and derivation efficiency of AG-haESCs between our and reported data (Yang et al., 2012). Data are represented as means ± SEM (n = 3 independent experiments).

(G) Representative images of colony morphologies (left), telomere signaling (middle), and G-binding karyotype (right) of indicated AG-haESCs. Scale bars, 100 μm.

(H) Immunofluorescent staining of indicated pluripotency markers in AG-haESC line A129-2 and AOS-14. Scale bars, 50 μm.

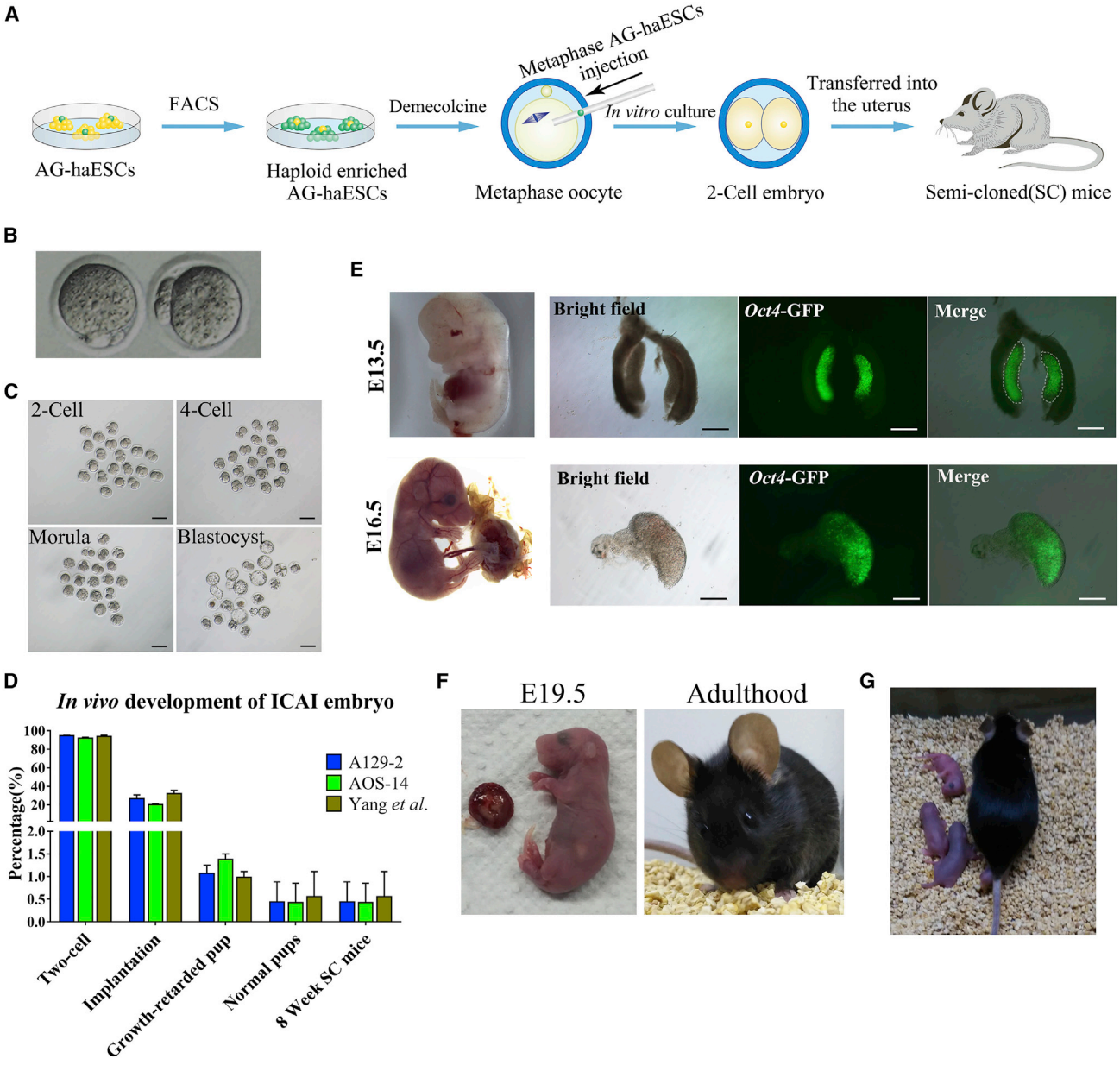

Figure 2. Developmental Potency of ICAI Embryos by AG-haESCs

(A) Schematic diagram of generating SC mice.

(B) Pseudopolar body was excluded several hours after ICAI embryos were activated.

(C) *In vitro* development of ICAI embryos by using AOS-14. Scale bars, 100 μm.

(D) Comparison of *in vitro* and *in vivo* development efficiency between our and reported data (Yang et al., 2012). Data are represented as means ± SEM (n = 2 independent experiments).

(E) SC fetus showing *Oct4*-GFP signaling in the gonad and ovary at E13.5 and E16.5, respectively. Scale bars, 50 μm.

(F) Full-term (E19.5) and adulthood SC mice produced from AOS-14 AG-haESCs.

(G) SC mice can deliver offspring after mating with C57 male mouse.

We next analyzed the AG-haESC methylation levels in repetitive sequences and in DMRs. The bisulfite sequencing analysis indicated that major satellite repeats (pericentric repeats) in the A129-2 and AOS-14 cell lines decreased by 42.34% and 39.37% compared with 2n ESC (XX), respectively (Figures 4F and S4F). In addition, the methylation levels of minor satellite repeats (centric repeats) decreased by 43.33% in the A129-2 cells and 31.67% in the AOS-14

Please cite this article in press as: He et al., Reduced Self-Diploidization and Improved Survival of Semi-cloned Mice Produced from Androgenetic Haploid Embryonic Stem Cells through Overexpression of..., Stem Cell Reports (2018), https://doi.org/10.1016/j.stemcr.2017.12.024

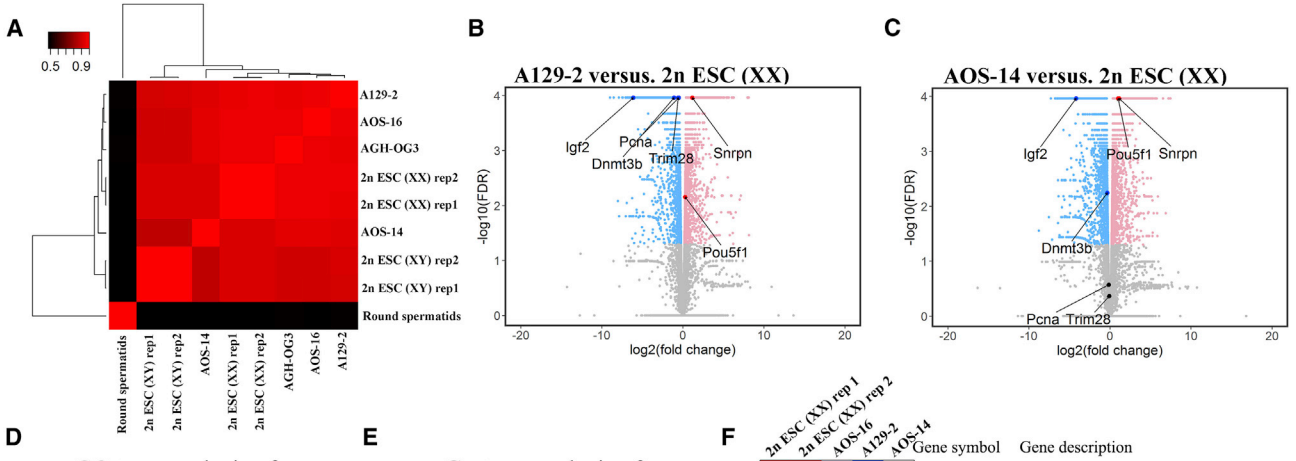

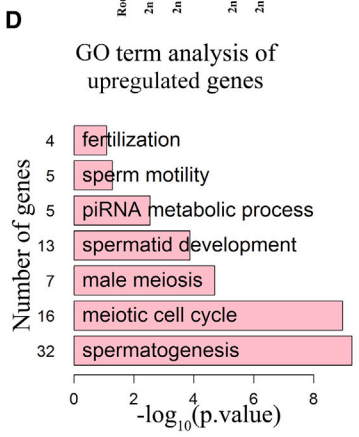

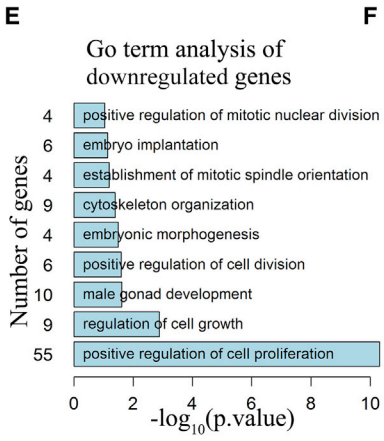

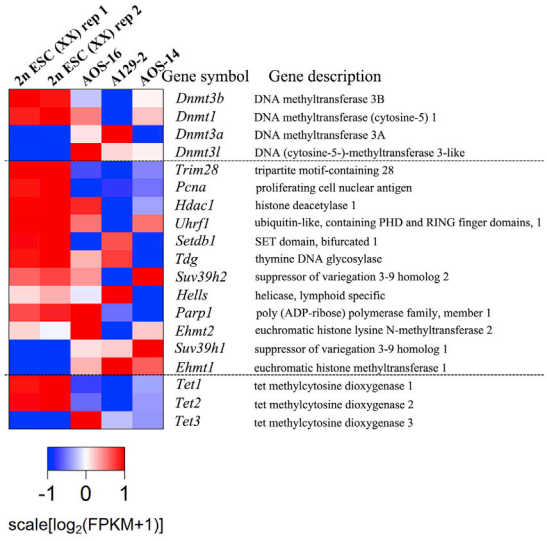

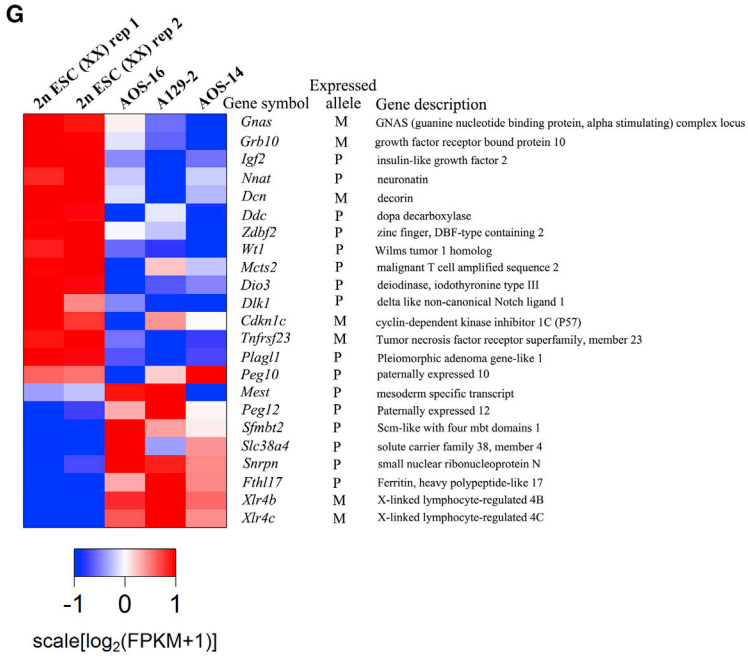

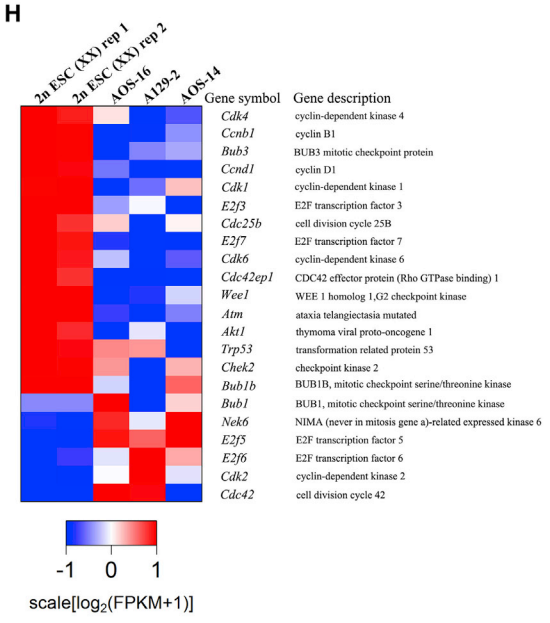

(legend on next page)

cells (Figures 4F and S4G). Moreover, both the A129-2 cells (reduced by 42.12% in IAP and 16.67% in LINE-1) and the AOS-14 cells (reduced by 41.15% in IAP and 15% in LINE-1) showed decreased methylation levels in their IAP and LINE-1 elements compared with 2n ESC (XX) (Figures 4F, S4H, and S4I). To note, almost every CpG site exhibited the reduced methylation pattern (Figures 4G and S4F–S4I). Interestingly, although the withdrawal of 2i increased the total amount of 5 mC in AG-haESCs (Figure S4B), only the methylation level of LINE-1 recovered to that of 2n ESC (XX) (Figures 4F, S4E, and S4I). In addition, upregulation of DNA methylation was noticed in restricted CpG sites (Figures S4C–S4I). Furthermore, self-diploidization was accelerated and cell proliferation was slowed down in both our and reported AG-haESCs (Yang et al., 2012) after withdrawal of 2i (Figures S4J and S4K). In addition, a severe loss of methylation in the DMRs of both *H19* and *Gtl2* was detected (Figures 4H and 4I), which is consistent with previous reports (Li et al., 2012; Yang et al., 2012). In contrast, the DMR of *Rasgrf1* was almost fully methylated (99%–100%) (Figure S4L).

Next, to determine why *Dnmt3b* was downregulated in the AG-haESCs, we performed bisulfite sequencing on its promoter region. There was no significant difference between the AG-haESCs and the 2n ESC (XX) (Figure S4M). Unexpectedly, chromatin immunoprecipitation (ChIP) analysis of histone modifications indicated a significantly reduced enrichment of the H3K4me1 and H3k27ac signals on the promoter as well as on the gene body of *Dnmt3b* (Figures 4J and S4N).

Methylation Recovery of AG-haESCs by *Dnmt3b* Overexpression

We speculated whether the rescue of DNMT3B expression could restore the abnormal phenotypes observed in the AG-haESCs. Overexpression of *Dnmt3b* was performed in the A129-2 cell line (A129-2#3b) using a lentiviral-based doxycycline (Dox)-inducible system (Gao et al., 2013). After Dox induction (72 hr), DNMT3B expression could reach a 2n ES-like level (Figure 5A). Moreover, genomic 5 mC level increased more than three times, but it was still lower than that of 2n ESCs (Figure 5B). IF staining further confirmed this result (Figures 5C and 5D). Excitingly, the methylation levels in those hypomethylated repetitive sequences as well as in the individual CpG sites were mostly recovered to a certain extent, similar to those of 2n ESC (XX) when DNMT3B was sufficient (Figures 5E, S5A, and S5B). More specifically, the methylation levels in major satellite, minor satellite, IAP, and LINE-1 in A129-2#3b (+Dox) were upregulated to 49.75%, 38.33%, 44.24%, and 22.33%, respectively (Figures 5E, S5A, and S5B).

Reduced Self-Diploidization by *Dnmt3b* Overexpression

We next asked whether *Dnmt3b* overexpression had any effects on self-diploidization and/or the AG-haESC cell cycle. Surprisingly, the self-diploidization of AG-haESCs was significantly alleviated by *Dnmt3b* overexpression (Figures 5F and S5C). Whether tested in the beginning after flow cytometry sorting or during the culturing process, Dox treatment for only 72 hr could effectively reduce the self-diploidization rate of the AG-haESCs (Figures 5F and S5D). Moreover, this effect could last up to 2 months, even after Dox withdrawal subsequent to a 72 hr Dox treatment (Figure S5E). Although ectopic *Dnmt3b* expression did not appear to alter cell proliferation (Figure S5F), qPCR analysis indicated certain genes that function in the G2/M transition that were obviously downregulated (Figure 5G). However, this effect could be counteracted by 5-aza-2′-deoxycytidine (5-AZA) treatment (Figures 5H and 5I). In addition, the enrichment of DNA methylation on these genes was confirmed by RRBS (reduced representation bisulfite sequencing) (Figure S5G). In addition, bromodeoxyuridine analysis suggested that the cell-cycle profile was different before and after Dox treatment, and there are more haploid ESCs remaining in *Dnmt3b*-overexpressed cells (Figure S5H).

To further confirm whether these functions were dependent on the catalytic activity of Dnmt3b, a catalytically

Figure 3. Transcriptome of AG-haESCs

(A) Hierarchical clustering of gene expression profiles based on Pearson correlation coefficient in A129-2, AOS-14, AOS-16, 2n ESC (XX), public 2n ESC (XY) (GSE93238), and reported AG-haESC line AGH-OG3 (GSE60072) (Zhong et al., 2015), as well as round spermatids. Colors from black to red indicate weak to strong correlation.

(B and C) Volcano plot shows gene expression changes between AG-haESCs, A129-2 (B) and AOS-14 (C), and 2n ESCs (XX). The light blue dots represent the genes that were significantly downregulated in AG-haESCs, while pink and gray dots represent the significantly upregulated genes and genes without significant change, respectively. The dots with deepened colors are genes of interest. FDR, false discovery rate.

(D and E) Significantly enriched GO terms for upregulated genes (D) and downregulated genes (E) in AG-haESCs compared with 2n ESC (XX).

(F–H) Heatmap shows expression of methylation- and demethylation-related genes (F), imprinted genes (G), and cell-cycle-related genes (H) in 2n ESC (XX) and indicated AG-haESC lines. For comparison, original gene expression values in fragments per kilobase of transcript per million mapped reads (FPKM) were subjected to logarithmic transformation followed by center scale normalization in each sample and then scaled to the range of −1 to 1 for each gene across all samples. The gene names and descriptions are indicated on the right.

Please cite this article in press as: He et al., Reduced Self-Diploidization and Improved Survival of Semi-cloned Mice Produced from Androgenetic Haploid Embryonic Stem Cells through Overexpression of..., Stem Cell Reports (2018), https://doi.org/10.1016/j.stemcr.2017.12.024

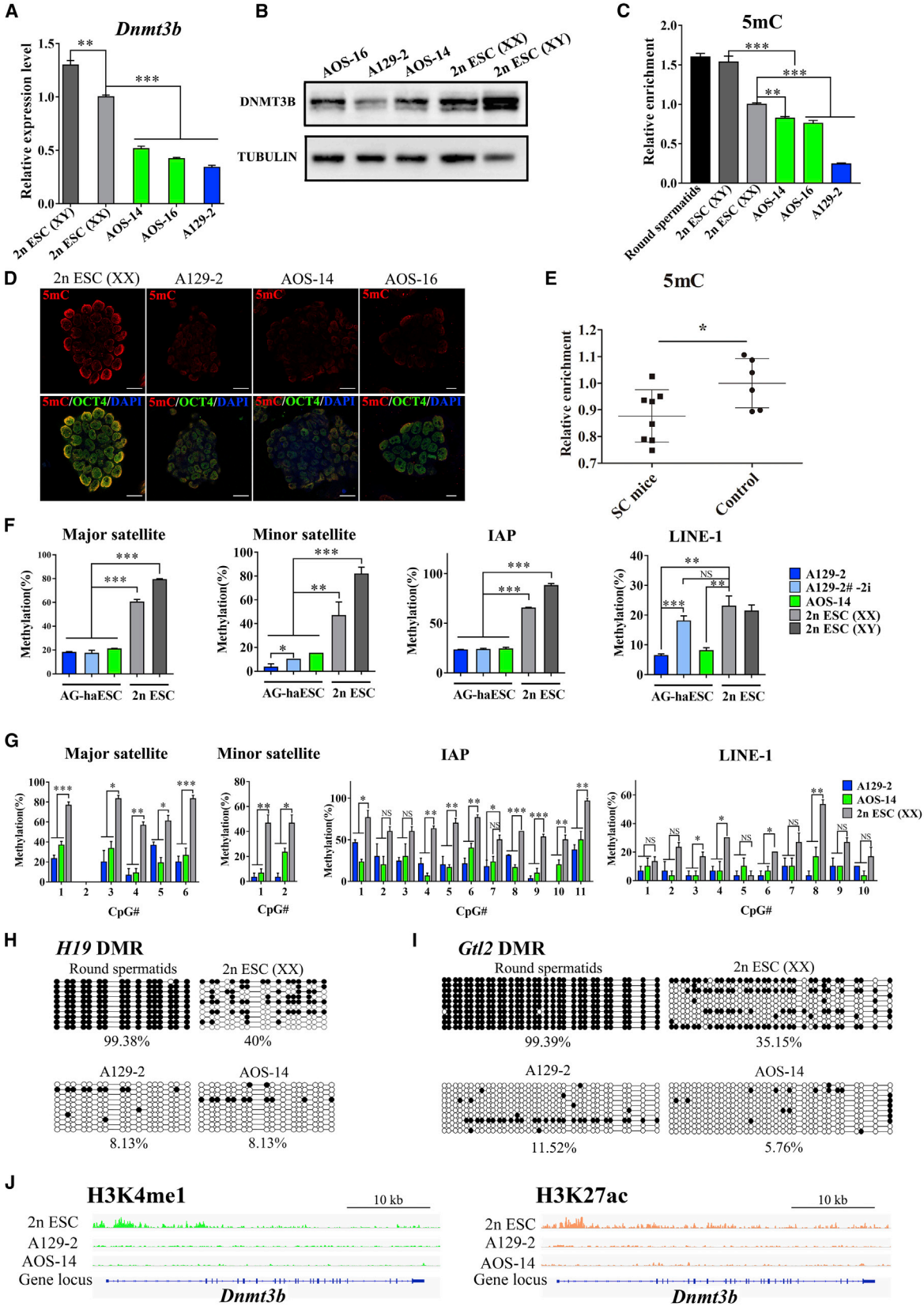

(legend on next page)

dead version of Dnmt3b (V725G), referred to as A129-2#3b_mut, was ectopically expressed in the AG-haESCs. The result indicated that no 5 mC recovery could be detected (Figure S5I). Moreover, self-diploidization was slightly accelerated (Figure S5J) and certain cell-cycle genes (*Chek2*, *Cdk1*, *Wee1*, and *Bub3*) were upregulated in A129-2#3b_mut cells (Figure S5K).

In addition, we were surprised to find that the paternally expressed genes *Igf2* and *U2af1-rs1* were upregulated and the maternally expressed genes *Gtl2* and *Snrpn* were downregulated after *Dnmt3b* overexpression, which were previously abnormally expressed (Figures 5J, S5L, and S5M). Moreover, the methylation level in the distal CTCF binding region (−32 kb to *H19* transcription start site) of the *H19/Igf2* locus was increased by more than 2-fold (Figure S7E). Nevertheless, *Dnmt3b* overexpression seemed to have no apparent effect on the detected DMRs of *H19* and *Gtl2* (Figure S5N).

Derivation of AG-haESCs Was Severely Impaired When *Dnmt3b* Was Deficient

Considering overexpression of *Dnmt3b* could rescue certain dysfunctions observed in hypomethylated AG-hESCs, we further determined whether *de novo* DNA methylation was essential for the derivation of AG-haESCs by applying both siRNA technology and the CRISPR/Cas9 system. The results showed that only one AG-haESC line, referred to as AG-haESC#3b KO (knockout), could be finally established from initial 323 *Dnmt3b* KO embryos, and the derivation efficiency was obviously lower compared with the control group (Figures 6A–6C and S6A). In addition, Sanger sequencing and western blot analysis both confirmed the deficiency of *Dnmt3b* (Figures S6B and S6C). Despite that an AG-ESC line (AG-ESC#3a KO) could be generated when *Dnmt3a* was deficient, the *in vitro* development of *Dnmt3a* KO embryos was significantly reduced (Figures 6D and S6A), and no haploid cell line could be successfully established (Figures 6E, 6F, S6A, and S6D). Collectively, these results clearly suggested that *Dnmt3b* as well as *Dnmt3a* was essential for the development of AG haploid embryos and derivation of AG-haESCs.

Dnmt3b Overexpression Improved the Survival of SC Mice Produced from DKO AG-haESCs

We next investigated whether overexpression of *Dnmt3b* and the subsequent genomic methylation recovery had functional effects on AG-haESCs. The results demonstrated that the efficiency for the *in vitro* development of ICAI blastocysts and implantation rate of transplanted embryos was significantly increased to 64.95% and 51.07%, respectively (Figures 7A, 7B, and S7A). Moreover, the survival rate of A129-2#3b (+Dox) SC mice increased to 10.14% at E15.5 (Figures 7A, 7B, and S7A). However, the further birth rate is not promoted. Thus, other defects such as abnormal imprinted genes like *H19*, *Igf2*, and *Gtl2* should be further rescued as was done in DKO AG-haESCs.

We then took advantage of a DKO AG-haESC line, which was previously proven to greatly improve SC mice generation (Zhong et al., 2015). Similar to that observed in wild-type AG-haESCs, the DKO AG-haESCs showed genome-wide hypomethylation and were recovered when *Dnmt3b* was ectopically expressed (Figures 7C–7E). In addition, reduced self-diploidization, suppressed cell-cycle-related genes, and further rescued expression of certain

Figure 4. Methylation Analysis of AG-haESCs

(A) Validation of *Dnmt3b* expression in indicated cell lines by real-time qPCR. The expression level was normalized by *Gapdh* and compared with that observed in 2n ESC (XX) (n = 3 independent experiments).

(B) Western blot analysis of DNMT3B in indicated cell lines. β-TUBULIN was used as an endogenous control.

(C) 5 mC level in indicated cells as analyzed by UHPLC-MRM-QQQ analysis. The results were normalized to that in 2n ESC (XX). All the ESCs were cultured in the 2i-containing medium (n = 3 independent experiments).

(D) Reduced 5 mC signaling in indicated AG-haESCs compared with 2n ESC (XX) by IF staining. Scale bars, 20 μm.

(E) SC mice generated from AG-haESCs showing lower frequency of 5 mC. Genomic DNA was extracted from the body of fetuses at E14.5–E16.5. The control indicates the E14.5–E16.5 fetuses produced by natural mating. Each dot represents the 5 mC content of a single mouse. The results were normalized to those in control fetuses. Data are represented as the means ± SD (n = 6–8 mice; 5 independent experiments).

(F) Bisulfite sequencing analysis of major satellite, minor satellite, LINE-1, and IAP in indicated cell lines. A129-2, AOS-14, 2n ESC (XX), and 2n ESC (XY) were cultured with 2i addition, whereas A129-2# −2i cells were cultured without 2i (n = 10 single DNA molecules; 3 independent experiments).

(G) Summary of the methylation changes in indicated cell lines. The horizontal axis represents the individual CpG sites. The vertical axis represents the percentage of methylated cytosines (n = 10 single DNA molecules; 3 independent experiments).

(H and I) A129-2 and AOS-14 show hypomethylation at DMRs of *H19* (I) and *Gtl2* (J) by bisulfite analysis. Open and closed circles indicate unmethylated and methylated CpGs, respectively.

(J) H3K4me1 and H3K427ac ChIP-sequencing peaks at *Dnmt3b* gene loci in indicated cells.

Data in (A), (C), (F), and (G) are represented as the means ± SEM. *p < 0.05; **p < 0.01; ***p < 0.001 by Student's t test for comparison. NS, not significantly different.

Please cite this article in press as: He et al., Reduced Self-Diploidization and Improved Survival of Semi-cloned Mice Produced from Androgenetic Haploid Embryonic Stem Cells through Overexpression of..., Stem Cell Reports (2018), https://doi.org/10.1016/j.stemcr.2017.12.024

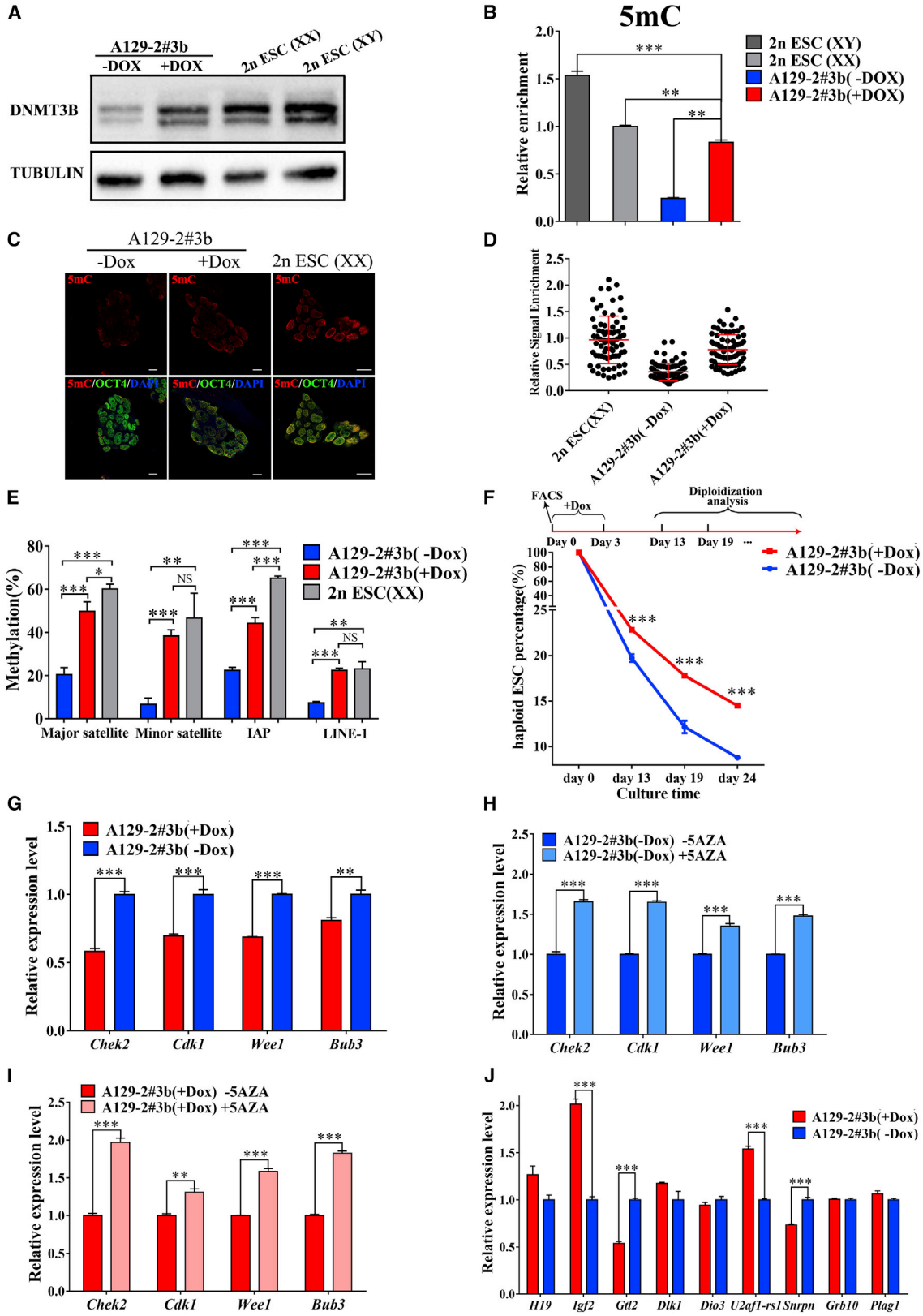

(legend on next page)

imprinted genes were noticed in DKO AG-haESC#3b (+Dox) (Figures S7B–S7D). Moreover, the methylation in the distal CTCF binding region of the *H19/Igf2* locus was also partially recovered (Figures S7E and S7F). Excitingly, the survival rate of newborn full-term SC mice was remarkably improved using DKO AG-haESC#3b after Dox treatment, while the birth rate was not altered (Figures 7F–7H). Of the 31 full-term SC mice produced from DKO AG-haESC#3b (+Dox), 3 were cannibalized by the lactating mother, while 28 mice (90%) survived to adulthood (8 weeks) and grew normally during the 9-month observation period. As a comparison, almost 50% of the SC mice died within 1 month of using hypomethylated DKO AG-haESC#3b (−Dox) as the donor cells (Figures 7F and 7H). In addition, certain imprinted genes were mis-regulated in these DKO SC mice that died shortly after birth (Figure 7I). More importantly, only DKO SC#3b (+Dox) mice showed a rescued expression pattern of *Igf2*, while other genes were recovered in the remaining live adult DKO SC mice (Figure 7J).

DISCUSSION

In this study, we established six AG-haESC lines from two genetic backgrounds, which all showed pluripotency and differentiation potential comparable to those of 2n mESCs (Figures 1C, 1H, and S1F–S1I). In addition, the A129-2 and AOS-14 cells could replace sperm to produce full-term, alive SC mice (Figure 2D). RNA-seq analysis demonstrated that the AG-haESCs simultaneously expressed pluripotent- and gamete-related genes, which fully explains their dual functions (Figures 3D, S3C, and S3D). In addition, it is interesting to find that both female cells (X and XX) showed higher expression of *Nanog* and *Oct4* compared with 2n ESC (XY), which was in accordance with recent studies indicating that female ESCs are closer molecularly to the naive state (Figure S3D) (Choi et al., 2017a, 2017b). Moreover, AG-haESCs also exclusively upregulated several naive pluripotent genes (Figure S3C). However, certain methylation-, imprinted-, and cell-cycle-related genes showed obvious abnormal expression patterns, which may account for the low efficiency of SC mice production as well as the high self-diploidization rate observed in the AG-haESCs (Figures 3F–3H and S3G).

Global hypomethylation was found in our and reported AG-haESCs (Figures 4C, 4D, and 7C–7E) (Zhong et al., 2015). Moreover, methylation reduction occurred at almost every CpG site in certain repetitive sequences and DMRs of imprinted genes (Figures 4G–4I and S4F–S4I). Interestingly, despite AG-haESCs showing upregulated 5 mC level when cultured without 2i (Figure S4B), recovery of DNA methylation occurred only in restricted CpG sites (Figures S4C–S4I). In addition, two recent studies have shown that 2n ESC (XX) exhibited imprinting control region demethylation regardless of culture conditions (Choi et al., 2017b; Yagi et al., 2017). However, different from those reported deficiencies in 2n ESC (XX), recently established mouse AG-haESCs and parthenogenetic haESCs, which could give birth to SC mice, were all derived and maintained in a 2i system (Li et al., 2012, 2016; Yang et al., 2012; Zhong et al., 2016a).

Figure 5. A129-2#3b (+Dox) AG-haESCs Show Recovered DNA Methylation and Reduced Self-Diploidization

(A) Western blot analysis of DNMT3B in indicated cell lines. β-TUBULIN was used as an endogenous control.

(B) Upregulated 5 mC level in genomic DNA of A129-2#3b (+Dox) AG-haESCs. The results were normalized to those in 2n ESC (XX) (n = 3 independent experiments).

(C) IF staining of 5 mC in A129-2#3b AG-haESCs with (+) and without (−) Dox treatment. 2n ESC (XX) was set as a control. Scale bars, 20 μm.

(D) Relative enrichment of 5 mC signals in indicated cell lines. Each point represents the relative fluorescence intensity of a nucleus in indicated cell lines. The results were normalized to those in 2n ESC (XX). Data are represented as the means ± SD (n > 70 single nuclei).

(E) Bisulfite sequencing analysis of methylation in repetitive sequences of A129-2#3b AG-haESCs with (+) and without (−) Dox treatment. 2n ESC (XX) was set as a control (n = 10 single DNA molecules; 3 independent experiments).

(F) Self-diploidization analysis in indicated A129-2#3b AG-haESCs (n = 5 independent experiments).

(G) Validation of indicated cell-cycle-related genes in A129-2#3b with (+) and without (−) Dox treatment. The expression level was normalized by *Gapdh* and compared with that observed in A129-2#3b (−Dox) (n = 3 independent experiments).

(H) Validation of indicated cell-cycle-related genes in A129-2#3b(−Dox) with (+) and without (−) 72 hr 5-AZA treatment. The expression level was normalized by *Gapdh* and compared with that observed in A129-2#3b (−Dox) −5-AZA (n = 3 independent experiments).

(I) Validation of indicated cell-cycle-related genes in A129-2#3b (+Dox) with (+) and without (−) 72 hr of 5-AZA treatment. The expression level was normalized by *Gapdh* and compared with that observed in A129-2#3b (+Dox) −5-AZA (n = 3 independent experiments).

(J) Validation of imprinted genes in indicated cell lines by real-time qPCR. The expression level was normalized by *Gapdh* and compared with that observed in A129-2#3b (−Dox) (n = 3 independent experiments).

Data in (B) and (E)–(J) are represented as the means ± SEM. *p < 0.05; **p < 0.01; ***p < 0.001 by Student's t test for comparison. Cells in (A)–(J) were cultured under 2i-containing medium.

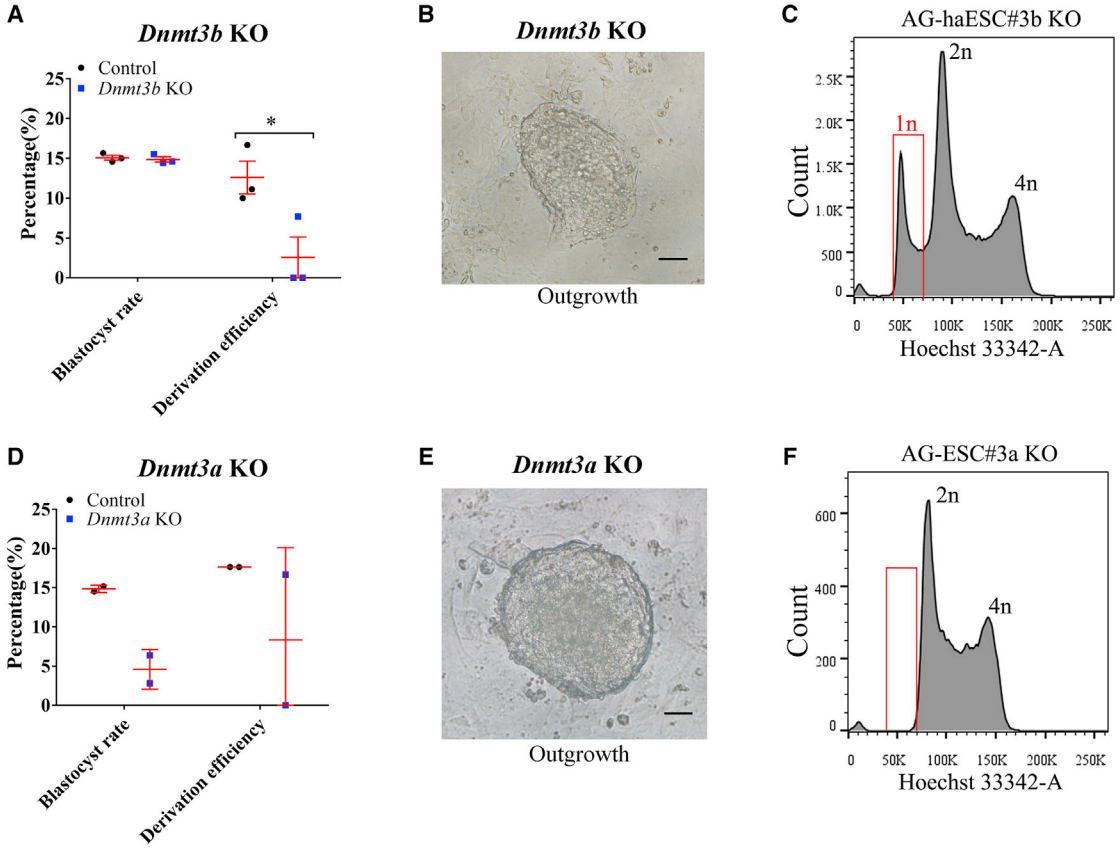

Figure 6. Derivation of AG-haESCs Was Severely Impaired When Dnmt3b Was Deficient

(A) *In vitro* development efficiency of androgenetic haploid embryos and derivation efficiency of androgenetic ESC in *Dnmt3b* KO and control groups. Data are represented as the means ± SD (n = 3 independent experiments). *p < 0.05 by Student's t test for comparison.

(B) Outgrowth derived from a *Dnmt3b* KO androgenetic blastocyst. Scale bar,100 μm.

(C) The presence of haploid cells (indicated as 1n) in AG-haESC#3b KO cells shown by flow chart.

(D) *In vitro* development efficiency of androgenetic haploid embryos and derivation efficiency of androgenetic ESC *Dnmt3a* KO and control groups. Data are represented as the means ± SD (n = 2 independent experiments).

(E) Outgrowth derived from a *Dnmt3a* KO androgenetic blastocyst. Scale bar,100 μm.

(F) The absence of haploid cells in AG-ESC#3a KO cells shown by flow chart.

Low expression of *Dnmt3b* and aberrant expression of other methylation-related genes might be the main cause of DNA hypomethylation in the wild-type and DKO AG-haESCs (Figures 3F, 4A–4C, S4A, and 7C–7E). However, deficient *Dnmt3b* and hypomethylation appeared to have no distinctive effects on the pluripotent properties of the AG-haESCs, which was consistent with those observed in the *Dnmt3b*$^{-/-}$ and Dnmt triple-KO 2n ESCs (Okano et al., 1999; Tsumura et al., 2006). Even though the male pronucleus undergoes demethylation after fertilization, hypomethylation of spermatozoa is not feasible (Benchaib et al., 2005; Takashima et al., 2009). In addition, embryogenesis is severely impaired when *Dnmt3b* is homozygously deleted (Okano et al., 1999). Here, we further demonstrated that the derivation of AG-haESCs was severely impaired when Dnmt3b was deficient (Figures 6A and S6A). In addition, no AG-haESC line from *Dnmt3a* KO embryos could be successfully established (Figures 6F and S6A), which in all suggested that proper content of methylation was essential for the development of AG haploid embryos and derivation of AG-haESCs.

In the present study, hypomethylation was noticed in both wild-type and DKO AG-haESCs (Figures 4C and 7C), which may further influence the embryonic development and/or survival of SC mice. Moreover, mutations in human DNMT3B have been reported to cause a rare autosomal-recessive disorder characterized by genome-wide hypomethylation and multiradiate chromosomes (Jin et al., 2008; Okano et al., 1999). In addition, inactivation of *Dnmt3b* or reduced methylation in mammalian somatic cells could result in global DNA hypomethylation, premature senescence, and chromosomal instability (Dodge et al.,

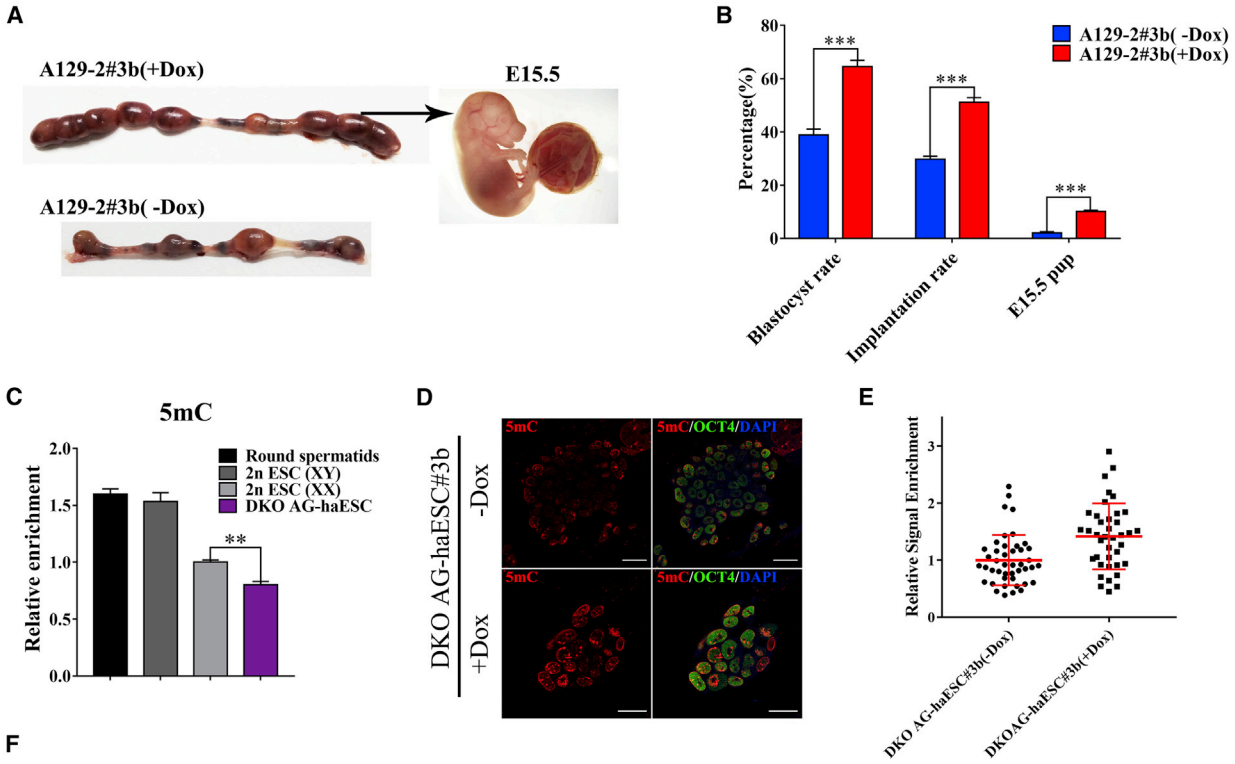

F

ES cell line	Replicates	No. of manipulated	No. of 2-Cell (%)	Transferred embryo stage	No. of recipient	No. of normal pups (% of transferred embryo)	No. of pups surviving to 8 week(% of normal pups)
DKO AG-haESC#3b(+DOX)	1	118	112(94.92)	two-cell embryo	3	11(9.82)	9 (81.82)
	2	136	127(93.38)	two-cell embryo	3	13(10.24)	13(100)
	3	71	66 (92.96)	two-cell embryo	2	7 (10.61)	6 (85.71)
	Subtotal	325	305(93.85)		8	31(10.61)	28(90.32)
DKO AG-haESC#3b(-DOX)	1	160	153(95.63)	two-cell embryo	4	14(9.15)	7 (50)
	2	94	86 (91.49)	two-cell embryo	2	9 (10.46)	4 (44.44)
	3	167	161(96.41)	two-cell embryo	4	18(11.18)	10(55.56)
	Subtotal	421	400(95.01)		10	41(10.25)	21(51.22)

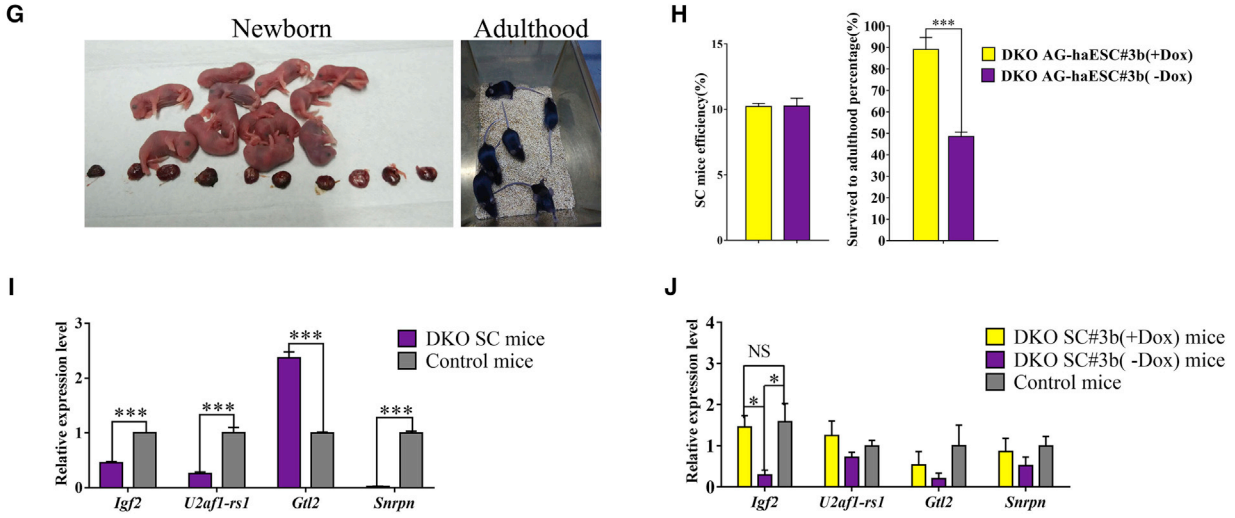

(legend on next page)

2005; Jackson-Grusby et al., 2001; Walsh et al., 1998; Xu et al., 1999). These results may partially explain the low survival rate observed in the full-term SC mice generated from both wild-type and DKO AG-haESCs (Figures 4E, 7C, and 7H). In addition, DNA hypomethylation and aberrant imprinting expression were inherited in the generated SC mice (Figures 4C–4E, S5L, S5M, and 7I) (Li et al., 2012; Yang et al., 2012).

Overexpression of *Dnmt3b* could partially restore global methylation content and increase 5 mC in hypomethylated repetitive sequences in the AG-haESCs (Figures 5B–5E, 7D, and 7E). Importantly, methylation in the distal CTCF binding region of the *H19/Igf2* locus was recovered 2-fold after *Dnmt3b* overexpression, which can further help to block the combination of the insulator CTCF protein so that the downstream enhancer can activate the *Igf2* promoter more efficiently (Figures 5J, S7D, and S7E) (Lee and Bartolomei, 2013; Plasschaert and Bartolomei, 2014). In addition, recovered expression of *Gtl2*, *Snrpn,* and *U2af1-rs1* was also determined (Figures 5J and S7D). It should be noted that proper expression of certain imprinted genes has been shown to be essential for the generation and survival of SC mice (Li et al., 2016; Yang et al., 2012; Zhong et al., 2015). Moreover, the methylation pattern in hypomethylated repetitive sequences was recovered to a 2n ESC (XX) like state after *Dnmt3b* overexpression, which is consistent with the reported function of *Dnmt3b* (Figures 5E, S5A, and S5B) (Kato et al., 2007).

Surprisingly, the self-diploidization of AG-haESCs was significantly mitigated by the transient overexpression of *Dnmt3b* (Figures 5F and S5C–S5E), and certain G2/M-related genes were downregulated (Figure 5G). In addition, we further demonstrated that these genes could be regulated by DNA methylation in AG-haESCs (Figures 5H, 5I, and S5G). Moreover, a recent study also proved a role of Dnmt3b in regulating *Chek2* expression through promoter methylation (Sheikh et al., 2017). In all, our result was consistent with several previous reports that shortening mitosis or promoting the G2/M transition could efficiently reduce AG-haESC self-diploidization (He et al., 2017; Kalitsis et al., 2000; Matsuoka et al., 1998; Pierce et al., 1998; Takahashi et al., 2014; Zhu et al., 2004). In addition, the *Dnmt3b*-mediated methylation recovery in major and minor satellites could also be a reason for the reduced self-diploidization of AG-haESCs (Figures 5E, S5A, and S5B), as centromeres that contain pericentric major satellite repeats and centric minor satellite repeats are key elements for centromeric cohesion and the segregation of sister chromatids (Guenatri et al., 2004). Similarly, a recent report showed that self-diploidization of haploid ESCs can be slowed by overexpression of Aurora B, which plays a role in correct chromosome alignment and segregation during mitosis (Guo et al., 2017).

In summary, our study provides direct evidence that overexpression of *Dnmt3b* can restore the methylation status of hypomethylated AG-haESCs, mitigate self-diploidization, improve developmental potential of ICAI embryos, and significantly increase the survival rate of DKO SC mice. Regulation of other methylation-related genes might be important to further rescue the methylation levels of AG-haESCs and to increase the birth rates of SC mice. Moreover, whether *Dnmt3b* functions in parthenogenetic haESCs or primate haploid ESCs should be fully explored in future studies.

Figure 7. Improved Survival of SC Mice by Using DKO AG-haESC with Transient Overexpression of *Dnmt3b*

(A) Representative implantation sites and E15.5 pup produced from A129-2#3b with (+) and without (−) Dox treatment.

(B) Developmental potency of reconstructed ICAI embryos by A129-2#3b AG-haESCs with (+) and without (−) Dox treatment (n = 3 independent experiments).

(C) Lower frequency of 5 mC in DKO AG-haESC by UHPLC-MRM-QQQ analysis. The result was normalized to that in 2n ESC (XX) (n = 3 independent experiments).

(D) IF staining of 5 mC in DKO AG-haESC#3b with (+) and without (−) Dox treatment. Scale bars, 20 μm.

(E) Relative enrichment 5 mC signals in DKO AG-haESC#3b with (+) and without (−) Dox treatment. Each point represents the relative fluorescence intensity of a nucleus in indicated cell lines. The results were normalized to those in DKO AG-haESC#3b (−Dox). Data are represented as the means ± SD (n > 35 single nuclei).

(F) *In vivo* development potential of ICAI embryos by using DKO AG-haESC#3b with (+) or without (−) Dox treatment as donor cells.

(G) Representative DKO AG-haESC#3b (+Dox) SC mice at E19.5 (indicated as newborn) and 3 months (indicated as adulthood).

(H) Comparison of the birth rate (left) of full-term SC mice and survival rate (right) of SC mice with 3 months observation by using indicated donor cells (n = 3 independent experiments).

(I) Expression of indicated imprinted genes in SC mice (produced by DKO AG-haESC#3b [−Dox]), which died shortly after birth. Control represents the full-term female mice delivered after natural mating (n = 5 mice; 3 independent experiments).

(J) Expression of indicated imprinted genes in adult DKO SC#3b (+Dox) mice (produced by DKO AG-haESC#3b [+Dox]), DKO SC#3b (−Dox) mice (produced by DKO AG-haESC#3b [−Dox]), and control mice (wild-type C57 females). The RNA was extracted from the tail of adult mice (n = 5–9 mice; 3 independent experiments).

Data in (B), (C), and (H)–(J) are represented as the means ± SEM. *p < 0.05; **p < 0.01; ***p < 0.001 by Student's t test for comparison. NS, not significantly different.

EXPERIMENTAL PROCEDURES

Animal Use and Care

The specific-pathogen-free-grade mice, including 129Sv, C57BL/6 (*Oct4*-GFP transgenic) (Gao et al., 2013), ICR, and BDF1 mice, were housed in the animal facility at Tongji University. All the mice had free access to food and water. All the experiments were performed in accordance with the University of Health Guide for the Care and Use of Laboratory Animals and were approved by the Biological Research Ethics Committee of Tongji University.

Derivation of the AG-haESCs

The injection of sperm into enucleated oocytes was conducted as previously described (Yang et al., 2012). The blastocysts were planted on feeders in 15% KSR Knockout DMEM supplemented with 2i: 1 μM PD0325901 (Selleck) and 3 μM CHIR99021 (Selleck). After 6–8 days in culture, the outgrowths were passaged and cultured on feeders using 2i containing ES medium. ES medium contains DMEM (Merck Millipore) supplemented with 15% (v/v) fetal bovine serum (HyClone), 1 mM L-glutamine (Merck Millipore), 0.1 mM mercaptoethanol (Merck Millipore), 1% nonessential amino acid stock (Merck Millipore), penicillin/streptomycin (100×, Merck Millipore), nucleosides (100×, Merck Millipore), and 1,000 U/mL LIF (Merck Millipore).

ACCESSION NUMBERS

The RNA-seq datasets (GEO: GSE99588), RRBS datasets (GEO: GSE107359), and ChIP-seq datasets (GEO: GSE107358) reported in this paper have been deposited in the NCBI Gene Expression Omnibus.

SUPPLEMENTAL INFORMATION

Supplemental Information includes Supplemental Experimental Procedures, seven figures, and three tables and can be found with this article online at https://doi.org/10.1016/j.stemcr.2017.12.024.

AUTHOR CONTRIBUTIONS

W.H., J.C., C.J., and S.G. conceived and designed the study. W.H. performed most of the experiments. Y.J. performed the G-banding karyotype. Z.X. and R.L. conducted telomere fluorescence *in situ* hybridization. H.L. Wang, W. Lai, and C.L. performed UHPLC-MRM-QQQ analysis. X.Z. and W.Z. did most of the bioinformatic analysis. W.H., W. Liu, X.K., and Y.Z. performed the microinjection. Z.X., M.C., J.Y., M.W., K.Z., and Z.Q. participated in plasmid construction and FACS. Y.Z., H.W., and L.Z. performed the bisulfite sequencing assay and western blot. X.H. performed the ChIP experiments. R.X., H. Wang, X.W., C.L., and Z.H. participated in other mice-related experiments, real-time qPCR, and data analysis. W.H., J.C., and S.G. wrote the paper.

ACKNOWLEDGMENTS

We thank Professor J.S. Li for sharing AG-haESCs and C.X. Chen for assistance with FACS. This work was primarily supported by the National Key R&D Program of China (2016YFA0100400) and the National Natural Science Foundation of China (31721003). This work was also supported by the Ministry of Science and Technology of China (2014CB964803 and 2015CB964800), the National Natural Science Foundation of China (81630035, 31401247, 31501196, 31501183, and 31501197), the Shanghai Subject Chief Scientist Program (15XD1503500), the Shanghai Chenguang Program (16CG17, 16CG19, and 15CG19), the Shanghai municipal medical and health discipline construction projects (no. 2017ZZ02015), and the Fundamental Research Funds for the Central Universities (2000219145).

Received: July 13, 2017
Revised: December 29, 2017
Accepted: December 29, 2017
Published: January 25, 2018

REFERENCES

Benchaib, M., Braun, V., Ressnikof, D., Lornage, J., Durand, P., Niveleau, A., and Guérin, J.F. (2005). Influence of global sperm DNA methylation on IVF results. Hum. Reprod. *20*, 768–773.

Bird, A. (2002). DNA methylation patterns and epigenetic memory. Genes Dev. *16*, 6–21.

Choi, J., Clement, K., Huebner, A.J., Webster, J., Rose, C.M., Brumbaugh, J., Walsh, R.M., Lee, S., Savol, A., Etchegaray, J.P., et al. (2017a). DUSP9 modulates DNA hypomethylation in female mouse pluripotent stem cells. Cell Stem Cell *20*, 706–719.e7.

Choi, J., Huebner, A.J., Clement, K., Walsh, R.M., Savol, A., Lin, K., Gu, H., Di Stefano, B., Brumbaugh, J., Kim, S.Y., et al. (2017b). Prolonged Mek1/2 suppression impairs the developmental potential of embryonic stem cells. Nature *548*, 219–223.

Crichton, J.H., Dunican, D.S., Maclennan, M., Meehan, R.R., and Adams, I.R. (2014). Defending the genome from the enemy within: mechanisms of retrotransposon suppression in the mouse germline. Cell. Mol. Life Sci. *71*, 1581–1605.

Dodge, J.E., Okano, M., Dick, F., Tsujimoto, N., Chen, T., Wang, S., Ueda, Y., Dyson, N., and Li, E. (2005). Inactivation of Dnmt3b in mouse embryonic fibroblasts results in DNA hypomethylation, chromosomal instability, and spontaneous immortalization. J. Biol. Chem. *280*, 17986–17991.

Elling, U., Taubenschmid, J., Wirnsberger, G., O'Malley, R., Demers, S.P., Vanhaelen, Q., Shukalyuk, A.I., Schmauss, G., Schramek, D., and Schnuetgen, F. (2011). Forward and reverse genetics through derivation of haploid mouse embryonic stem cells. Cell Stem Cell *9*, 563–574.

Gao, Y., Chen, J., Li, K., Wu, T., Huang, B., Liu, W., Kou, X., Zhang, Y., Huang, H., and Jiang, Y. (2013). Replacement of Oct4 by Tet1 during iPSC induction reveals an important role of DNA methylation and hydroxymethylation in reprogramming. Cell Stem Cell *12*, 453–469.

Guenatri, M., Bailly, D., Maison, C., and Almouzni, G. (2004). Mouse centric and pericentric satellite repeats form distinct functional heterochromatin. J. Cell Biol. *166*, 493–505.

Guo, A., Huang, S., Yu, J., Wang, H., Li, H., Pei, G., and Shen, L. (2017). Single-cell dynamic analysis of mitosis in haploid

embryonic stem cells shows the prolonged metaphase and its association with self-diploidization. Stem Cell Reports *8*, 1124–1134.

He, Z.Q., Xia, B.L., Wang, Y.K., Li, J., Feng, G.H., Zhang, L.L., Li, Y.H., Wan, H.F., Li, T.D., Xu, K., et al. (2017). Generation of mouse haploid somatic cells by small molecules for genome-wide genetic screening. Cell Rep. *20*, 2227–2237.

Hirasawa, R., Chiba, H., Kaneda, M., Tajima, S., Li, E., Jaenisch, R., and Sasaki, H. (2008). Maternal and zygotic Dnmt1 are necessary and sufficient for the maintenance of DNA methylation imprints during preimplantation development. Genes Dev. *22*, 1607–1616.

Jackson-Grusby, L., Beard, C., Possemato, R., Tudor, M., Fambrough, D., Csankovszki, G., Dausman, J., Lee, P., Wilson, C., Lander, E., et al. (2001). Loss of genomic methylation causes p53-dependent apoptosis and epigenetic deregulation. Nat. Genet. *27*, 31–39.

Jin, B., Tao, Q., Peng, J., Soo, H.M., Wu, W., Ying, J., Fields, C.R., Delmas, A.L., Liu, X., Qiu, J., et al. (2008). DNA methyltransferase 3B (DNMT3B) mutations in ICF syndrome lead to altered epigenetic modifications and aberrant expression of genes regulating development, neurogenesis and immune function. Hum. Mol. Genet. *17*, 690–709.

Kalitsis, P., Earle, E., Fowler, K.J., and Choo, K.H. (2000). Bub3 gene disruption in mice reveals essential mitotic spindle checkpoint function during early embryogenesis. Genes Dev. *14*, 2277–2282.

Kato, Y., Kaneda, M., Hata, K., Kumaki, K., Hisano, M., Kohara, Y., Okano, M., Li, E., Nozaki, M., and Sasaki, H. (2007). Role of the Dnmt3 family in de novo methylation of imprinted and repetitive sequences during male germ cell development in the mouse. Hum. Mol. Genet. *16*, 2272–2280.

Kaufman, M.H., Robertson, E.J., Handyside, A.H., and Evans, M.J. (1983). Establishment of pluripotential cell lines from haploid mouse embryos. J. Embryol. Exp. Morphol. *73*, 249–261.

Lane, N., Dean, W., Erhardt, S., Hajkova, P., Surani, A., Walter, J., and Reik, W. (2003). Resistance of IAPs to methylation reprogramming may provide a mechanism for epigenetic inheritance in the mouse. Genesis *35*, 88–93.

Lee, J.T., and Bartolomei, M.S. (2013). X-inactivation, imprinting, and long noncoding RNAs in health and disease. Cell *152*, 1308–1323.

Leeb, M., Walker, R., Mansfield, B., Nichols, J., Smith, A., and Wutz, A. (2012). Germline potential of parthenogenetic haploid mouse embryonic stem cells. Development *139*, 3301–3305.

Leeb, M., and Wutz, A. (2011). Derivation of haploid embryonic stem cells from mouse embryos. Nature *479*, 131–134.

Li, E., Bestor, T.H., and Jaenisch, R. (1992). Targeted mutation of the DNA methyltransferase gene results in embryonic lethality. Cell *69*, 915–926.

Li, W., Li, X., Li, T., Jiang, M.G., Wan, H., Luo, G.Z., Feng, C., Cui, X., Teng, F., Yuan, Y., et al. (2014). Genetic modification and screening in rat using haploid embryonic stem cells. Cell Stem Cell *14*, 404–414.

Li, W., Shuai, L., Wan, H., Dong, M., Wang, M., Sang, L., Feng, C., Luo, G.Z., Li, T., Li, X., et al. (2012). Androgenetic haploid embryonic stem cells produce live transgenic mice. Nature *490*, 407–411.

Li, Z., Wan, H., Feng, G., Wang, L., He, Z., Wang, Y., Wang, X.J., Li, W., Zhou, Q., and Hu, B. (2016). Birth of fertile bimaternal offspring following intracytoplasmic injection of parthenogenetic haploid embryonic stem cells. Cell Res. *26*, 135–138.

Martinez, J.G., Perez-Escuredo, J., Castro-Santos, P., Marcos, C.A., Pendas, J.L., Fraga, M.F., and Hermsen, M.A. (2012). Hypomethylation of LINE-1, and not centromeric SAT-alpha, is associated with centromeric instability in head and neck squamous cell carcinoma. Cell. Oncol. (Dordr.) *35*, 259–267.

Matsuoka, S., Huang, M., and Elledge, S.J. (1998). Linkage of ATM to cell cycle regulation by the Chk2 protein kinase. Science *282*, 1893–1897.

Nichols, J., and Smith, A. (2011). The origin and identity of embryonic stem cells. Development *138*, 3–8.

Okano, M., Bell, D.W., Haber, D.A., and Li, E. (1999). DNA methyltransferases Dnmt3a and Dnmt3b are essential for de novo methylation and mammalian development. Cell *99*, 247–257.

Okano, M., Xie, S., and Li, E. (1998). Cloning and characterization of a family of novel mammalian DNA (cytosine-5) methyltransferases. Nat. Genet. *19*, 219–220.

Pierce, A.M., Schneider-Broussard, R., Philhower, J.L., and Johnson, D.G. (1998). Differential activities of E2F family members: unique functions in regulating transcription. Mol. Carcinog. *22*, 190–198.

Plasschaert, R.N., and Bartolomei, M.S. (2014). Genomic imprinting in development, growth, behavior and stem cells. Development *141*, 1805–1813.

Reik, W., Dean, W., and Walter, J. (2001). Epigenetic reprogramming in mammalian development. Science *293*, 1089–1093.

Sagi, I., Chia, G., Golan-Lev, T., Peretz, M., Weissbein, U., Sui, L., Sauer, M.V., Yanuka, O., Egli, D., and Benvenisty, N. (2016). Derivation and differentiation of haploid human embryonic stem cells. Nature *532*, 107–111.

Sheikh, M.A., Malik, Y.S., and Zhu, X. (2017). RA-induced transcriptional silencing of checkpoint kinase-2 through promoter methylation by Dnmt3b is required for neuronal differentiation of P19 cells. J. Mol. Biol. *429*, 2463–2473.

Takahashi, S., Lee, J., Kohda, T., Matsuzawa, A., Kawasumi, M., Kanai-Azuma, M., Kaneko-Ishino, T., and Ishino, F. (2014). Induction of the G2/M transition stabilizes haploid embryonic stem cells. Development *141*, 3842–3847.

Takashima, S., Takehashi, M., Lee, J., Chuma, S., Okano, M., Hata, K., Suetake, I., Nakatsuji, N., Miyoshi, H., Tajima, S., et al. (2009). Abnormal DNA methyltransferase expression in mouse germline stem cells results in spermatogenic defects. Biol. Reprod. *81*, 155–164.

Tsumura, A., Hayakawa, T., Kumaki, Y., Takebayashi, S., Sakaue, M., Matsuoka, C., Shimotohno, K., Ishikawa, F., Li, E., Ueda, H.R., et al. (2006). Maintenance of self-renewal ability of mouse embryonic stem cells in the absence of DNA methyltransferases Dnmt1, Dnmt3a and Dnmt3b. Genes Cells *11*, 805–814.

Walsh, C.P., Chaillet, J.R., and Bestor, T.H. (1998). Transcription of IAP endogenous retroviruses is constrained by cytosine methylation. Nat. Genet. *20*, 116–117.

Wutz, A. (2014). Haploid animal cells. Development *141*, 1423–1426.

Xu, G.L., Bestor, T.H., Bourc'his, D., Hsieh, C.L., Tommerup, N., Bugge, M., Hulten, M., Qu, X., Russo, J.J., and Viegas-Péquignot, E. (1999). Chromosome instability and immunodeficiency syndrome caused by mutations in a DNA methyltransferase gene. Nature *402*, 187–191.

Yagi, M., Kishigami, S., Tanaka, A., Semi, K., Mizutani, E., Wakayama, S., Wakayama, T., Yamamoto, T., and Yamada, Y. (2017). Derivation of ground-state female ES cells maintaining gamete-derived DNA methylation. Nature *548*, 224–227.

Yan, H., Yuan, J., Gao, L., Rao, J., and Hu, J. (2016). Long noncoding RNA MEG3 activation of p53 mediates ischemic neuronal death in stroke. Neuroscience *337*, 191–199.

Yang, H., Liu, Z., Ma, Y., Zhong, C., Yin, Q., Zhou, C., Shi, L., Cai, Y., Zhao, H., Wang, H., et al. (2013). Generation of haploid embryonic stem cells from Macaca fascicularis monkey parthenotes. Cell Res. *23*, 1187–1200.

Yang, H., Shi, L., Wang, B.A., Liang, D., Zhong, C., Liu, W., Nie, Y., Liu, J., Zhao, J., Gao, X., et al. (2012). Generation of genetically modified mice by oocyte injection of androgenetic haploid embryonic stem cells. Cell *149*, 605–617.

Yi, M., Hong, N., and Hong, Y. (2009). Generation of medaka fish haploid embryonic stem cells. Science *326*, 430–433.

Ying, Q.L., Wray, J., Nichols, J., Batlle-Morera, L., Doble, B., Woodgett, J., Cohen, P., and Smith, A. (2008). The ground state of embryonic stem cell self-renewal. Nature *453*, 519–523.

Zhong, C., Xie, Z., Yin, Q., Dong, R., Yang, S., Wu, Y., Yang, L., and Li, J. (2016a). Parthenogenetic haploid embryonic stem cells efficiently support mouse generation by oocyte injection. Cell Res. *26*, 131–134.

Zhong, C., Yin, Q., Xie, Z., Bai, M., Dong, R., Tang, W., Xing, Y.H., Zhang, H., Yang, S., Chen, L.L., et al. (2015). CRISPR-Cas9-mediated genetic screening in mice with haploid embryonic stem cells carrying a guide RNA library. Cell Stem Cell *17*, 221–232.

Zhong, C., Zhang, M., Yin, Q., Zhao, H., Wang, Y., Huang, S., Tao, W., Wu, K., Chen, Z.J., and Li, J. (2016b). Generation of human haploid embryonic stem cells from parthenogenetic embryos obtained by microsurgical removal of male pronucleus. Cell Res. *26*, 743–746.

Zhu, W., Giangrande, P.H., and Nevins, J.R. (2004). E2Fs link the control of G1/S and G2/M transcription. EMBO J. *23*, 4615–4626.

Zvetkova, I., Apedaile, A., Ramsahoye, B., Mermoud, J.E., Crompton, L.A., John, R., Feil, R., and Brockdorff, N. (2005). Global hypomethylation of the genome in XX embryonic stem cells. Nat. Genet. *37*, 1274–1279.